JAST, Vol. 3, No. 3, pp 159–166

JAST
Journal of Aerospace Science and Technology

RESEARCH NOTE

Laminar and Turbulent Aeroheating Predictions around Multi-Cone Configurations in Hypersonic Equilibrium-Air Flow

H. Parhizkar[1], S. M. H. Karimian[2]

This paper is devoted to aerodynamic heating calculation of the axisymmetric bodies with discontinuities in the surface slope. The combined inviscid-boundary layer method is used to calculate laminar and turbulent aerodynamic heating of perfect gas and equilibrium air in hypersonic flow. In the existing approximate aeroheating codes, flow properties on the boundary layer edge are calculated from an approximate inviscid solution. This approach limits the application of such methods to simple blunt cones at low angle of attacks. In this paper, properties of boundary layer edge are calculated from an Euler solution. Due to a more accurate inviscid flow calculation, this method can be applied to a broader range of geometries, e.g. multi-cone configurations. Resulted aeroheating data from the present approach are compared with experimental data and found to be in good agreement under laminar and turbulent conditions. These include accurate predictions of aeroheating over the multi-cone bodies, which prove high capability of the method for this type of configurations.

NOMENCLATURE

EQ	Equilibrium air conditions
h	Enthalpy
M	Mach number
N	Turbulent velocity profile exponent
pr	Prandtl number
P	pressure
PG	Perfect gas conditions
q	Surface heat flux
r	Axisymmetric body radius
R	Recovery factor
R_n	Nose radius
Re	Reynolds number
s, n	Body fitted coordinate system
T	Temperature
u, v	Velocity component in the body fitted coordinate system
ω_f	Weighting function in transition region
$\bar{x}$	Ratio of the axial coordinate to the nose radius
α	Angle of attack
δ^*	Boundary layer displacement thickness
θ	Boundary layer momentum thickness
ρ	Density
μ	Viscosity

Subscripts

aw	Adiabatic wall
beg	Beginning of transition region
e	Boundary layer edge
end	End of transition region
L	Laminar
n	Nose
T	Turbulent
w	Wall
∞	Free stream condition

1. *Ph.D Candidate, Aerospace Department, Amirkabir University of Technology, Tehran, Iran, E-mail: hparhiz@aut.ac.ir.*
2. *Professor, Aerospace Department, Amirkabir University of Technology, Tehran, Iran, E-mail: hkarim@aut.ac.ir.*

INTRODUCTION

The thermal design of hypersonic vehicles requires accurate and reliable prediction of convective heat transfer over the surface of these vehicles. Due to the excessive CPU time and memory required for these predictions by a CFD approach, this approach may become impractical for the preliminary design environment where a range of geometries and flow parameters are to be studied. According to Prandtl's theory, there exists a thin boundary layer in fluid flow with small viscosity that includes viscous effects of flow [1]. Out of this thin layer, flow can be assumed to be inviscid.

One approach is to solve the inviscid flowfield first, and then to use the properties on the body surface as the edge conditions for a boundary layer solution. In this decoupled approach, the viscous layer is assumed to have a negligible effect on the outer inviscid region. This assumption is accurate for relatively high Reynolds number flows where the boundary layer is thin [2]. Euler equations may be solved for the inviscid part; however any simplification in the solution of the inviscid part can reduce the computational time. In 1964, Maslen [3, 4] introduced a simple inverse method to calculate the inviscid flowfield within the shock layer surrounding a simple axisymmetric cone, in which based on a prescribed shock shape, body shape is determined. Riley and DeJarentte modified Maslen's method to calculate surface pressures of the body, more accurately [5, 6]. The required CPU time and memory of the Maslen method and its modified version are much less than those required for an Euler solution, but the application of this method is limited to windward surface of the simple cones with blunt nose in hypersonic flows [3-8]. However, it should be noted that Euler solution gives the proper inviscid flow properties for more complex bodies.

The classical boundary layer equations can be solved to calculate the flow parameters and convective heat transfer rates in the viscous region. This heat transfer rate, which determines aerodynamic heating on the body surface, however, has been calculated by others [7-13] using Zoby's approximate convective-heating relations [14]. With Zoby's equations, the CPU time of calculation and the required memory are decreased significantly. Based on our experiment, the accuracy of the inviscid solution is a crucial parameter in calculation of boundary layer properties, e.g. convective heat transfer. In addition to this, a more accurate inviscid solution allows you to extend the calculation to geometrically complex bodies. In the present approach we suggest that the Euler solution can be used in combination with the Zoby's approximate convective-heating equations. With this combination, we are able to analyze aerodynamic heating of complex geometries. In the next section the solution scheme is presented.

SOLUTION SCHEME

In the present approach the inviscid flowfield should be solved first. This solution can be obtained using commercial codes or other existing Euler codes. All of the required properties on the body surface, including pressure, temperature and slip velocity components, that have been obtained from the Euler solution, are stored as the edge conditions for the solution of boundary layer equations; i.e. Zoby's equations. These equations are obtained from the integral form of the axisymmetric boundary layer momentum equation [15]. As shown in Figure 1, a body-fitted orthogonal coordinate system is chosen such that the origin of it is at the tip of the blunt nose, its s-axis is aligned with the surface and its n-axis is normal to the surface.

Applying the reference enthalpy method [16] (for compressibility effects) and the Reynolds analogy [15] to the integral form of the momentum equation in this coordinate system, the approximate convective heating equations for the laminar flow is obtained as [14]:

$$q_{w\,L} = 0.22\,(\mathrm{Re}_{\theta\,L})^{-1}\left(\frac{\rho^*}{\rho_e}\right)\left(\frac{\mu^*}{\mu_e}\right)\rho_e\,u_e(h_{aw}-h_w)(pr_w)^{-0.6} \tag{1}$$

The parameters of ρ^* and μ^* are used to consider the compressibility effects. In fact, the compressible gas effects can be considered by evaluating these parameters

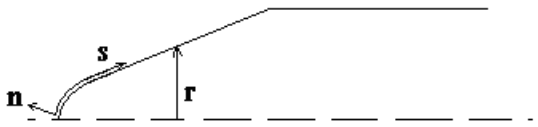

Figure 1. Coordinate system.

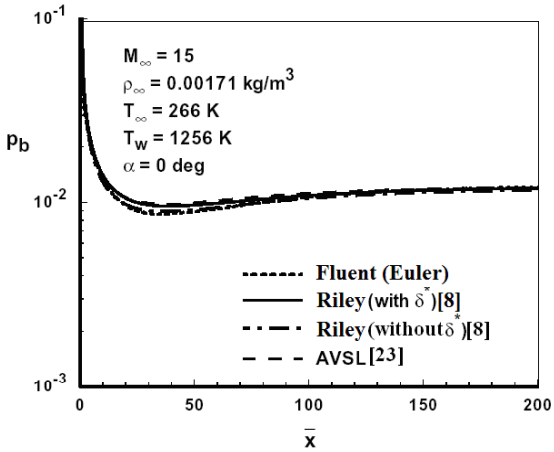

Figure 2. Body pressure comparison for 5 deg sphere-cone, $R_n = 0.0381m$.

at the Eckert's reference enthalpy [16] defined as:

$$h^* = 0.50h_e + 0.50h_w + 0.22R\frac{u_e^2}{2} \quad (2)$$

The momentum thickness Reynolds number is defined as:

$$\mathrm{Re}_{\theta_L} = \frac{\rho_e u_e \theta_L}{\mu_e} \quad (3)$$

The laminar boundary layer momentum thickness is calculated from the integration of the momentum equation along the surface coordinate [14]:

$$\theta_L = \frac{0.644[\int_0^s \rho^*\mu^* u_e\, r^2\, ds]^{1/2}}{\rho_e\, u_e\, r} \quad (4)$$

The adiabatic wall enthalpy is defined as:

$$h_{aw} = h_e + 0.5\ R\ u_e^2 \quad (5)$$

The recovery factor in the above equation is equal to $R \approx \mathrm{Pr}^{\frac{1}{2}}$ for the laminar flow and $R \approx \mathrm{Pr}^{\frac{1}{3}}$ for the turbulent flow [15]. Similar equations are developed for the turbulent flow [14]:

$$q_{w\,T} = c_1(\mathrm{Re}_{\theta T})^{-m}(\frac{\rho^*}{\rho_e})(\frac{\mu^*}{\mu_e})^m \rho_e\, u_e(h_{aw} - h_w)(pr_w)^{-0.4} \quad (6)$$

$$\theta_T = \frac{c_2\,[\int_0^s \rho^*\,\mu^{*^m}\,u_e\,r^{c_3}\,ds\,]^{c_4}}{\rho_e\,u_e\,r} \quad (7)$$

The coefficients of the m, c_1, c_2, c_3, and c_4 are functions of N, which is the exponent of the power-law turbulent velocity profile [14], and are given by:

$$m = \frac{2}{N+1}$$

$$c_1 = (\frac{1}{c_5})^{\frac{2N}{N+1}}\,[\frac{N}{(N+1)\,(N+2)}]^m$$

$$c_2 = (1+m)\,c_1, \quad c_3 = 1+m$$

$$c_4 = \frac{1}{c_3}, \quad c_5 = 2.2433 + 0.93N$$

A turbulent velocity profile of $u/u_e = (y/\delta)^{1/N}$ is assumed to calculate the required constants and exponents in the equations of momentum-thickness Reynolds number and the heat flux. Experimental results [17] show that N would be a function of Re_{θ_T}. Fitting a curve to the turbulent experimental data [14] produces the following equation:

$$N = 12.67 - 6.5\,Log(\mathrm{Re}_{\theta\,T}) + 1.21\,[\,Log(\mathrm{Re}_{\theta\,T})\,]^2 \quad (8)$$

As mentioned in Ref. 17, this formula is not suggested for Re_{θ_T} less than 10^4. Thus, to achieve more accurate aeroheating results for $\mathrm{Re}_{\theta_T} < 10^4$, we suggest that the 1/7 power law for velocity profile of the turbulent flat plate can be used.

In the transition region, both the laminar and turbulent values of heating rates, i.e. q_{W_L} and q_{W_T}, are calculated. Their distribution is then computed from the weighting function of Dhawan and Narasimha [18] as:
$q_W = q_{W_L} + \omega_f(q_{W_T} - q_{W_L})$ where $w_f = 1 - \exp(-0.412\xi_{tr}^2)$, $\xi_{tr} = 4(s - s_{beg})/(s_{end} - s_{beg})$. In the present approach, the beginning and the end of transition region must be specified.

For the perfect gas model, the viscosity is obtained using the Sutherland formula [15], and the specific heat ratio and Prandtl number are assumed to be the constant values of 1.4 and 0.71 for air, respectively. The thermal conductivity, however, is obtained from the definition of Prandtl number.

The mixture thermodynamic and transport properties of equilibrium chemically reacting air are provided in the form of tables. In this paper the thermodynamic properties of mixture enthalpy, $h(p,T)$, and density, $\rho(p,T)$, are interpolated from the tabular data of Tannehill and Mugge [19]. However, the transport properties of viscosity and thermal conductivity are interpolated from the tables provided by Hansen [20]. The Prandtl number is calculated using viscosity, thermal conductivity, and the mixture specific heat obtained through numerical differentiation of enthalpy data. In Ref. 21, it is shown that the Eckert's reference enthalpy formulation (Eq. 2) is still valid for equilibrium air. It should be noted that the values of ρ^* and μ^* must be evaluated at the thermodynamic properties of the Eckert's reference enthalpy (h^*) and the edge pressure (p_e) [21].

This completes the calculation procedure. Having known the values of pressure, temperature and the s-component of velocity at the edge of boundary i.e., P_e, T_e and u_e, the heating rate can be calculated on the surface of body, exposed by the no separated flows.

RESULTS AND DISCUSSION

In this section, results obtained from the present work are compared with available experimental data as well as with other approximate solutions.

Laminar Flow over the Blunt Cone (case 1)

The first test case corresponds to the laminar flow over a blunt cone at zero angle of attack. The cone half angle is 5 degrees and the nose radius is 0.0381m. Other flow parameters are as follows:

$M_\infty = 15, \quad \rho_\infty = 0.00171\,kg/m^3, \quad T_\infty = 266\,^o k,$

$T_w = 1256\,^o k, \quad \mathrm{Re}_{R_n} = 19000$

For the inviscid calculation, the domain is discretized into 4500 structured meshes. The calculated surface pressure distribution is compared with the other reliable results to ensure the inviscid solution accuracy. In the present approach, surface pressure distribution is the most effective parameter of the inviscid solution. As shown in Figure 2, two sets of Riley's results [8] are shown. The first set does not include the effect of the boundary layer displacement thickness (δ^*) on the inviscid flow region, however in the second set, the inviscid flow is calculated iteratively to include the δ^* effect. As seen earlier, the effect of δ^* appears somewhere between $25 < \bar{x} < 100$. In the other parts this effect is negligible.

As expected, the result of the Euler solution is in good agreement with the Riley's without δ^* result. Since we compare the present results with the available results such as approximate engineering methods, (e.g. Riley's method), the calculated pressure distribution is compared with the pressure distribution of Riley's method to show that they coincide with each other and therefore inviscid solution would not be a source of significant error in surface heat flux prediction of the present approach.

The surface heating rates are examined next in Figure 3. Results from the present approach are compared with heat-transfer data obtained from the Riley's and the AVSL methods. As shown, we have also presented the result obtained from the Fluent's FNS[3] solution.

FNS solution is obtained using 45000 structured cells. It takes 58 minutes to calculate FNS heating rates using a 2.8GHz Pentium-4 computer; however in the present approach, an Euler solution is obtained using 4500 structured cells in about 2 minutes by the same computer. For this test case, the viscous region solution (integration of the Zoby's equations) takes just less than 10 seconds.

In the first part, the present result matches the Riley's without δ^* result. In the downstream part of the body, however, the present result agrees very well with that of AVSL. It is noted that there is not much difference between two Riley's results. As a general view, in the first part, results of AVSL and Fluent are higher than the other results. However in the downstream part these two results converge to the result of the present approach. Therefore, in comparison with the available data, both present and Fluent results have good accuracy.

Low Reynolds Laminar Flow over the Blunt Cone (case 2)

In the second test, geometry and flow conditions are similar to the previous test case, except for the nose radius which is reduced to $R_n = 0.00381m$. The Inviscid surface pressure distribution in comparison

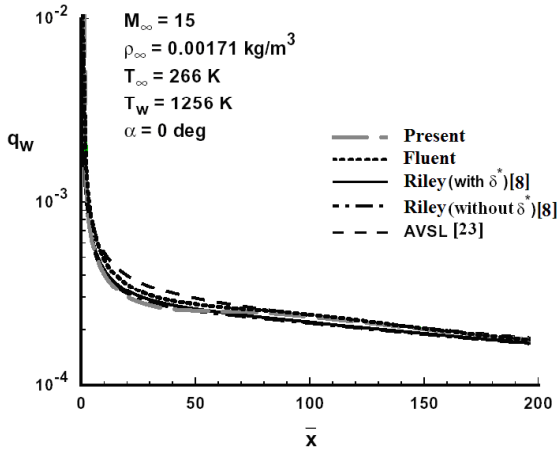

Figure 3. Heat transfer comparison for 5 deg sphere-cone, $R_n = 0.0381m$.

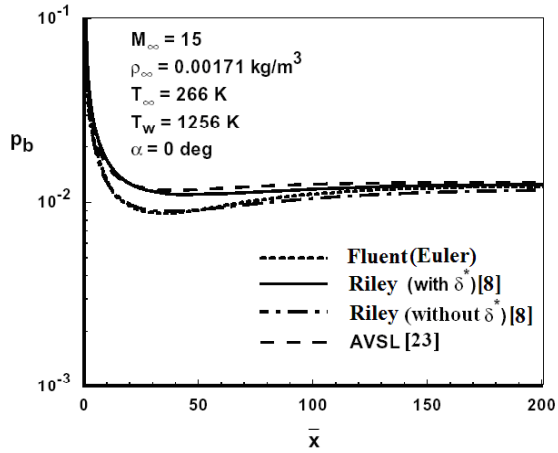

Figure 4. Body pressure comparison for 5 deg sphere-cone, $R_n = 0.00381m$.

with the other results is shown in Figure 4. As seen earlier, the result of the Euler solution is in good agreement with the Riley's without δ^* result. In the first test case it was shown that δ^* has a slight effect on surface pressure and heat flux distribution (see Figures. 2 and 3). In this test case, the Reynolds number is chosen to be 10 times smaller than the previous test case, i.e. $\mathrm{Re}_{R_n} = 1900$, in order to show the effect of δ^* growth. This effect is shown by Riley in Figure 4. As seen above, the surface pressure of Riley's with δ^* in the region of $10 < \bar{x} < 100$ has increased significantly due to the growth of the boundary layer thickness. In fact, by reducing the Reynolds number, the boundary layer displacement thickness has grown up and therefore the effective body has become thicker. This condition obviously changes the shock shape and the surface pressure.

The present surface heat flux is compared with the Riley's results and the AVSL results in Figure 5. This finding is in good agreement with the Riley's without δ^* result. Also note that the result of the Fluent is similar

to the AVSL result. A trend, similar to that happening in Figure 4, can be seen in Figure 5. The surface heat flux has increased in the region of $10 < \bar{x} < 100$ due to the effect of δ^*. As seen, even the Riley's with δ^* result has not predicted the correct heat flux increment. This fact had been previously seen in Figure 3.

Two comments should be made here. First, we can use the results of Fluent as the reference data in problems similar to the above cases. Second, Riley's method and also the present approach can not correctly predict the effect of boundary layer thickness. Nevertheless, the Riley's with δ^* method can slightly improve this drawback. In short, this is the penalty that is paid for the simplicity and the speed of the method to predict multi-cone heating rates.

Generally speaking, heat flux predictions of the present approach and Riley's method in Figure 5 are fairly good and acceptable in the aeroheating literature. Again we emphasize that at high Reynolds numbers the present approach has very high accuracy in predicting heat fluxes as shown in Figure 3. In the next test cases we consider the aeroheating prediction of multi-cone body surfaces.

Laminar Flow over the Cone-Cone Configuration (case 3)

All conditions of the third test case are similar to the first test case. The geometry, however, is changed as shown in Fig. 6. The calculated surface heat flux of this geometry in laminar flow is compared with the results of Fluent in Figure 7.

The predicted q_W on the first cone, is a little less than the result of Fluent, which is due to the δ^* effects. In the transient region between two cones, the predicted q_W is a little higher than the Fluent result. On the second cone, the surface heat flux is appropriately predicted. Small fluctuations seen in the result of Fluent at the rear part are because of the shock-boundary layer interaction. As stated earlier,

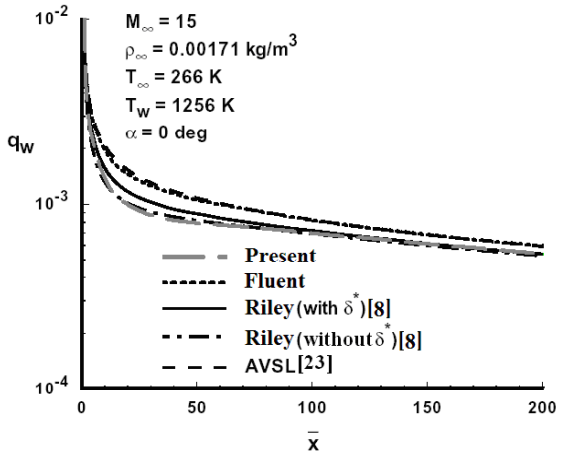

Figure 5. Heat transfer comparison for 5 deg sphere-cone, $R_{ne} = 0.00381m$.

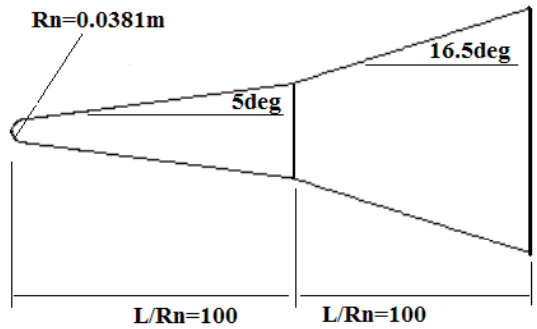

Figure 6. Double-cone body with the blunt nose.

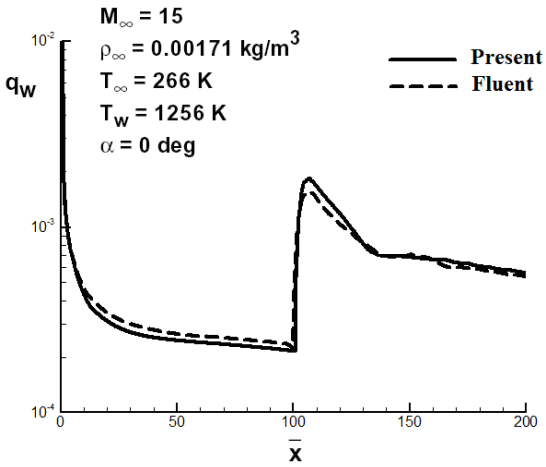

Figure 7. Heat transfer comparison for the double-cone body.

the present approach has well predicted surface heat flux of this double-cone geometry.

Laminar Flow over the Cone-cylinder–Cone Configuration (case 4)

In this test case, we consider the flow over a cone-cylinder-flare as shown in Figure 8. The flow condition is similar to the previous test case. The calculated surface heat flux distribution in comparison with the result of Fluent is shown in Figure 9. Similar to the previous test case, the predicted q_W on the first cone, agrees very well with the Fluent result. The expansion of the flow on the cylinder part causes reduction of the surface pressure. Thus, the boundary layer thickness is increased. As a result, the heat flux is decreased. As mentioned previously, a thicker boundary layer causes more errors, in heat flux prediction on the cylinder part. The deviation between the present results and Fluent's results in cylindrical part is due to this error. However, it should be stated that the accuracy of the present approach is very good in the conical parts and is appropriate on the cylinder part. As a first approximation, this is a very good result.

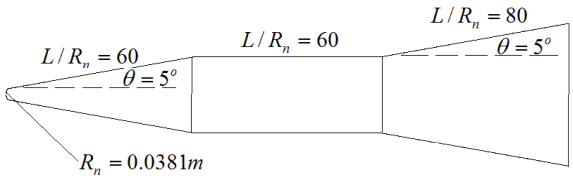

Figure 8. Cone-cylinder-flare configuration with the blunt nose.

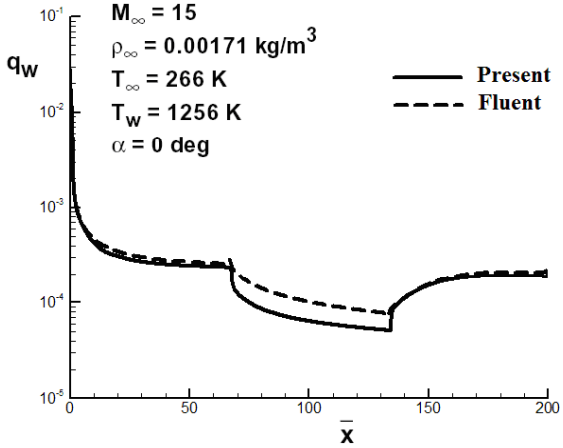

Figure 9. Heat transfer comparison for the cone-cylinder-flare body.

Turbulent Flow over the Blunt Cone (case 5)

The next test case is featured by turbulent flow calculation over a long, 5-deg sphere-cone at Mach 15. The nose radius is $R_n = 0.0381m$ and the solution is computed for a body with the length of $\bar{x} = 1125$. The free stream conditions are $p_\infty = 130.45pa$, $T_\infty = 263^o k$ and the wall temperature is $T_w = 1243^o k$. Computed surface heating rates are compared with the AVSL [24] and the VSL4 [25] results, in Figure 10.

In this figure, two sets of turbulent results are shown. In the first set, the exponent of the power-law turbulent velocity profile, N, is obtained from Ref. 14, in all ranges of Re_{θ_T}; however in the second set, the constant value of N=7 is only used for $\mathrm{Re}_{\theta_T} < 10^4$, as mentioned before. As discussed earlier, the accuracy of the results are improved very well when using this modification.

Based on the reported values of Ref. 24, the transition occurs from $\bar{x}_{beg} = 192$ to $\bar{x}_{end} = 450$. In comparison to the present approach and the method of VSL, the AVSL technique over-predicts the heating rates in downstream of the nose region, as shown in Figure 10. The approximation made in Maslen's pressure relation is the source of this deviation [25]. In fact, after the blunt section, in the beginning of the cone body where over-expansion occurs, the shock angle is quite different from the body angle. This fact, which happens in flow over long slender cones, is inconsistent with Maslen's assumption of a thin shock layer. We believe that using Euler solution for the calculation of surface pressure, which is employed in this paper, results in more accurate heating rates.

Transitional/Turbulent Flow with Equilibrium air conditions (case 6)

Surface heating rate over a 5 deg spherically blunted cone in equilibrium air with transitional/turbulent conditions is examined next. The results are compared with the heat transfer data obtained from the reentry flight test [26] and the Riley's results [8].

The freestream conditions are $M_\infty = 19.97$, $\rho_\infty = 0.0446\,kg/m^3$, $T_\infty = 221^o k$ and $\alpha = 0.14^o$, and the nose radius is 0.00356m. At the instance that the data are reported, the wall temperature varies from $604^o k$ in the nose tip to $431^o k$ in the end of the cone [27]. In this study we assume a linear variation of this wall temperature. Since the angle of attack is small, in this test case, the flowfield approximates our axisymmetric solver; i.e. α is assumed to be

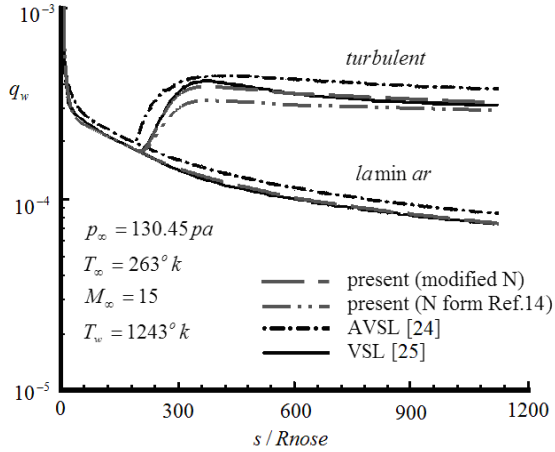

Figure 10. Heat transfer comparison for the turbulent flow over a long sphere-cone.

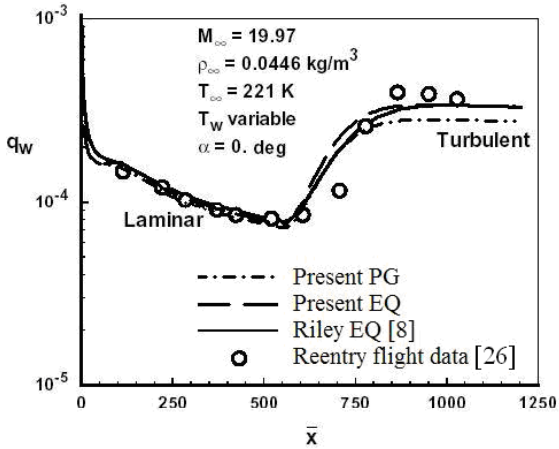

Figure 11. Heat transfer comparison for the transitional/turbulent equilibrium air flow over a long sphere-cone.

zero. Flow transition is assumed to be started at the reported distance of $\bar{x}_{beg} = 566$ [27]. As seen earlier, excellent agreement between the equilibrium results of the present approach and the fight data is noted, all over the body. These good results include both laminar and turbulent regions. The perfect gas results agree very well with the experimental data in the laminar flow, but slightly under-predicts the heating rate in the turbulent flow.

CONCLUSION

The present approach is proposed for the aeroheating calculation of the multi-cone configurations. Comparison of the present results with experimental data and the numerical results shows good accuracy of the present approach in prediction of aerodynamic heating. A critical study of the calculated results suggests that for more accurate results, the effect of boundary layer displacement thickness should be considered in the outer inviscid solution. Overall, with respect to the ability of the present approach in prediction of aerodynamic heating over the multi-cone configurations, the accuracy of the method is acceptable. It is noted that this accuracy is in the order of the accuracy of the existing approximate aeroheating methods.

ACKNOWLEDGMENTS

The authors are grateful to the Aerospace Department of Amirkabir University of Technology for their financial support.

REFERENCES

1. Anderson, J. D., *Hypersonic and High Temperature Gas Dynamics*, McGraw-Hill Book Company, New York, USA., (1989).
2. DeJarnette, F. R., Hamilton, H. H., Weilmuenster, K. J., and Cheatwood, F. M., "A Review of Some Approximate Methods Used in Aerodynamic Heating Analysis", *Journal of Thermophysics*, **1**(1), PP 5-12(1978).
3. Maslen, S. H., "Inviscid Hypersonic Flow Past Smooth Symmetric Bodies", *AIAA Journal*, **2**(6), PP 1055-1061(1964).
4. Maslen, S. H., "Asymmetric Hypersonic Flow", *NASA CR-2123*, (1972).
5. Riley, C. J., and DeJarnette, F. R., "An Approximate Method for Calculation Three-Dimensional Inviscid Hypersonic Flow Fields", *NASA TP-3018*, (1990).
6. Riley, C. J. and DeJarnette, F. R., "Engineering Calculations of Three-Dimensional Inviscid Hypersonic Flow Fields", *Journal of Spacecraft and Rockets*, **28**, PP 628-635(1991).
7. Riley, C. J. and DeJarnette, F. R., "Engineering Aerodynamic Heating Method for Hypersonic Flow", *Journal of Spacecraft and Rockets*, **2**, PP 327-334(1992).
8. Riley, C. J., "An Engineering Method for Interactive Inviscid-Boundary Layer in Three-Dimensional Hypersonic Flow", Ph.D. Thesis, North Carolina State University(1992).
9. Riley, C. J., Kleb, W. L., and Alter, S. J., "Aeroheating Predictions for X-34 Using an Inviscid-Boundary Layer Method", *AIAA Paper 98-0880*, (1998).
10. Hollis, B. R., and Horvath, T. J., "X-33 Computational Aeroheating Predictions and Comparisons with Experimental Data", *Journal of Spacecraft and Rockets*, **38**(3), PP 658-669(2001).
11. Zoby, E. V., Thompson, R. A., and Wurster, K. E., "Aeroheating Design Issues for Reusable Launch Vehicles-A Perspective", *AIAA Paper 2004-2535*, (2004).
12. Karimian, S. M. H., and Mahdizadeh, A., "Approximate Solution of Inviscid Flow around the Nose of Hypersonic Bodies at Angle of Attack", *Amirkabir Journal*, **12**(47), (2001).
13. Malekzadeh, M., Karimian, S. M. H., and Marefat, M., "An Engineering Inviscid-Boundary Layer Method for Calculation of Aerodynamic Heating in the Leeward Region", Proceedings of CFD2003, 11th Annual Conference of the CFD Society of Canada, Vancouver, Canada, (2003).
14. Zoby, E. V., Moss, J. J., and Sutton, K., "Approximate Convective-Heating Equations for Hypersonic Flows", *Journal of Spacecraft and Rockets*, **18**(1), PP 67-70(1981).
15. White, F. M., *Viscous Fluid Flow*, McGraw-Hill Book Company, New York, USA, (1974).
16. Eckert, E. R. G., "Engineering Relations for Friction and Heat Transfer to Surfaces in High Velocity Flow", *Journal of the Aeronautical Sciences*, **22**(8), PP 585-587(1955).
17. Johnson, C. B., and Bushnell, D. M., "Power-Law Velocity-Profile-Exponent Variations with Reynolds Number, Wall Cooling, and Mach Number in a Turbulent Boundary Layer", *NASA TN D-5753*, (1970).
18. Dhawan, S., and Narasimha, R., "Some Properties of Boundary Layer Flow During Transition from Laminar to Turbulent Motion", *Journal of Fluid Mechanics*, **3**, PP 418-436(1958).
19. Tannehill, J. C., and Mugge, P. H., "Improved Curve Fits for the Thermodynamic Properties of Equilibrium Air Suitable for Numerical Computer Using Time-Dependent or Shock-Capturing Methods", *NASA CR-2470*, (1974).
20. Hansen, C. F., "Approximations for the Thermodynamic and Transport Properties of High-Temperature Air", *NASA TN-4150*, (1958).
21. Simeonides, G., "Generalized Reference Enthalpy Formulations and Simulation of Viscous Effects in Hypersonic Flow", *Shock Waves*, **8**(3), PP 161-172(1998).
22. Dieudonne, W., Boerrigter, H. L., and Charbonnier, J. M., "Hypersonic Flow on a Blunted Cone-Flare and

in the VKI-H3 Mach 6 Wind Tunnel", von Karman Institute, TN-193, (1997).

23. Cheatwood, F. M., and DeJarnette, F. R., "Approximate Viscous Shock Layer Technique for Calculating Hypersonic Flows About Blunt-Nosed Bodies", *Journal of Spacecraft and Rockets*, **31**(4), PP 621-628(1994).
24. Grantz, A. C., DeJarnette, F. R., and Thompson, R. A., "Approximate Viscous Shock Layer Method for Hypersonic Flow Over Blunt-Nosed Bodies", *Journal of Spacecraft and Rockets*, **27**(6), PP 597-605(1990).
25. Gupta, R. N., Lee, K. P., Zoby, E. V., Moss, J. N., and Thompson, R. A., "Hypersonic Viscous Shock Layer Solution Over Long Slender Bodies- Part 1: High Reynolds Number Flows", *Journal of Spacecraft and Rockets*, **27**(2), PP 175-184(1990).
26. Stainback, P. C., Johnson, C. B., Boney, L. B., and Wicker, K. C., "Comparison of Theoretical Predictions and Heat Transfer Measurements for a Flight Experiment at Mach 20 (Reentry F)", *NASA TM X-2560*, (1972).
27. Bhutta, B. A., and Lewis, C. H., "Comparison of Hypersonic Experiments and PNS Predictions Part I: Aerothermodynamics", *Journal of Spacecraft and Rockets*, **28**(4), PP 376-386(1991).